Bilayers merge even when exocytosis is transient

Justin W. Taraska and Wolfhard Almers*

Vollum Institute, Oregon Health and Sciences University, 3181 Southwest Sam Jackson Park Road, Portland, OR 97239

Edited by Pietro V. De Camilli, Yale University School of Medicine, New Haven, CT, and approved April 27, 2004 (received for review February 25, 2004)

During exocytosis, the lumen of secretory vesicles connects with the extracellular space. In some vesicles, this connection closes again, causing the vesicle to be recaptured mostly intact. The degree to which the bilayers of such vesicles mix with the plasma membrane is unknown. Work supporting the kiss-and-run model of transient exocytosis implies that synaptic vesicles allow neither lipid nor protein to escape into the plasma membrane, suggesting that the two bilayers never merge. Here, we test whether neuroendocrine granules behave similarly. Using two-color evanescent field microscopy, we imaged the lipid probe FM4-64 and fluorescent proteins in single dense core granules. During exocytosis, granules lost FM4-64 into the plasma membrane in small fractions of a second. Although FM4-64 was lost, granules retained the membrane protein, GFP-phogrin. By using GFP-phogrin as a probe for resealing, it was found that even granules that reseal lose FM4-64. We conclude that the lipid bilayers of the granule and the plasma membrane become continuous even when exocytosis is transient.

PC12 cells | evanescent field microscopy | kiss-and-run | FM4-64

In many types of cells, exocytosis causes the membrane of a secretory vesicle to flatten into the cell surface and to release its components into the plasma membrane. It is now clear, however, that the membranous cavities of some vesicles reseal after exocytosis, thereby disconnecting the vesicles from the plasma membrane. The most direct evidence was obtained where exocytosis and resealing could be studied at the level of single vesicles, as was done in mast cell granules (1, 2), in endocrine granules (3–8), and in synaptic-like microvesicles of an endocrine gland (9). The resealing of secretory vesicles is thought to be advantageous to cells because it saves them the effort of retrieving vesicle membrane components by molecular sorting.

How far does fusion progress before a vesicle reseals? We consider two possibilities. In the first, fusion goes to completion and the bilayers of the fusing compartments merge. Now, the vesicle's membrane components may be free to leave, and their dispersal can be avoided only partially, and only if the vesicle reseals quickly. In the second, the lipid bilayers of the fusing compartments remain separate. Such fusion was observed when a viral envelope protein mediated cell–cell fusion, and when electric currents could pass between the fusing cells for minutes before fluorescent lipids could do so (10–12). During such incomplete fusion, it is thought that fusion-mediating proteins, such as viral envelope proteins or soluble *N*-ethylmaleimide-sensitive factor attachment protein receptors (SNAREs), may remain at the fusion site. There, they form a fusion pore that allows the exchange of water-soluble molecules, yet also constitute a fence (12) that prevents vesicle membrane components from leaving the vesicle.

Optical measurements of the loss of the styryl dye FM1-43 from synaptic vesicles in hippocampal neurons of mammals (13–18) and in motor neurons of flies (19) support a model in which vesicles can reseal. Indeed, the concept of resealing was first suggested for synaptic vesicles (20) where it has become known under the name "kiss-and-run" (21). If the retention of membrane components is the goal, then incomplete fusion seems advantageous, especially in synaptic vesicles where diffusion distances are smallest and membrane components would escape the fastest. Synaptic vesicles undergoing kiss-and-run were found to retain their entire store of the membrane protein synaptobrevin (18) although other authors differ on this point (22). Most importantly, synaptic vesicles were also found to retain half or more of the fluorescent lipid probe FM1-43 (17) even when they remained open to the external space for an entire second (15). In kiss-and-run, synaptic vesicles evidently reseal before their bilayers have merged with the plasma membrane (13, 17). After more conventional fusion, bilayers become continuous in milliseconds. This result was obtained by using FM1-43 in giant synaptic terminals from goldfish retinal bipolar cells (23).

Must one assume that exocytosis is reversible only as long as the lipid bilayers of vesicle and cell remain separate? Here, we determined in single vesicles how rapidly a fluorescent lipid escaped after exocytosis and whether that same vesicle later resealed. Single granules of PC12 cells were found to lose the lipid FM4-64 rapidly, regardless of whether or not they later resealed.

Methods

Plasmids, Solutions, and Cells. The neuropeptide Y (NPY)-enhanced GFP (EGFP) and EGFP-phogrin plasmids have been described (7, 24). Phogrin-monomeric red fluorescent protein (mRFP) was made by removing the ORF of EGFP by restriction digestion from the *Kpn*I/*Not*I sites in phogrin-EGFP (25) and replacing it with the ORF of mRFP (26). mRFP was a gift of R. Y. Tsien (University of California at San Diego, La Jolla). PC12-GR5 cell stocks were cultured as described (7). Briefly, cells were plated onto poly-L-lysine-coated high refractive index glass coverslips ($n_{488} = 1.80$, Plan Optik, Elsoff, Germany). Cells were transfected with 1 μg of plasmid DNA by using Lipofectamine 2000 (Invitrogen) according to the manufacturer's instructions and incubated for no less than 24 hr. In some experiments, cells were then incubated for an additional 12–24 hr in culture media containing 6.4 μM FM4-64. They were then thoroughly washed for 0.5–1 hr in dye-free media. For imaging, cells were maintained in imaging buffer (130 mM NaCl/2.8 mM KCl/5 mM $CaCl_2$/1 mM $MgCl_2$/10 mM Hepes/10 mM glucose, pH 7.4). To stimulate exocytosis, individual cells were depolarized by a 20- to 100-s-long local superfusion with elevated [K^+] from a micropipette (105 mM KCl/50 mM NaCl/2 mM $CaCl_2$/0.7 mM $MgCl_2$/1 mM NaH_2PO_4/10 mM Hepes, pH 7.4). The exocytic events analyzed herein occurred between 0.5 and 60 s after the start of perfusion. In some experiments, the perfusion with elevated [K^+] was immediately followed by a second perfusion with an imaging buffer wherein 50 mM NaCl was replaced by 50 mM NH_4Cl. In others, cells were ruptured by a strong jet of imaging solution through a pipette placed within a few micrometers of a cell. Experiments were carried out at room temperature (28°C).

This paper was submitted directly (Track II) to the PNAS office.

Abbreviations: EGFP, enhanced GFP; mRFP, monomeric red fluorescent protein; NPY, neuropeptide Y; $\Delta F/F$, fractional fluorescence change; SNARE, soluble *N*-ethylmaleimide-sensitive factor attachment protein receptor.

*To whom correspondence should be addressed. E-mail: almersw@ohsu.edu.

www.pnas.org/cgi/doi/10.1073/pnas.0401316101

Fluorescence Microscopy. Cells were imaged with an inverted microscope (IX-70; Olympus America, Melville, NY) configured for evanescent field excitation as described (7, 27, 28) and equipped with a 1.65 N.A. objective (Apo × 100 O HR, Olympus) and an image splitter (Multispec MicroImager, Optical Insights, Santa Fe, NM) for the simultaneous imaging of red and green fluorescent probes. Fluorescence was excited by an argon/krypton laser (Coherent Inc., Santa Clara, CA), usually at 488 nm and in some experiments (mRFP) simultaneously at 488 nm and 568 nm. Optical filters and dichroic mirrors were as in Merrifield *et al*. (28). The resulting green and red images were then projected side-by-side onto a back-illuminated charge-coupled device camera (Quantix 57, and Cascade 512 B for phogrin-mRFP, both from Roper Scientific, Trenton, NJ). Images were acquired by using METAMORPH software (Universal Imaging, Dowington, PA). For precise alignment of the red and green images, we took pictures of 200-nm fluorescent beads (Molecular Probes) fluorescing both red and green, and then proceeded as described (7). Pixel size was 61 nm. Frames were acquired as streams at 33 Hz, or in time-lapse recordings with 150-ms exposures given at 2 Hz. To adjust the polarization of the incident laser beam, a quarter wave plate was placed in the laser path and turned 45° to rotate the polarization of the laser from vertical to horizontal. Polarization direction was confirmed with an analyzer.

Image Analysis. For colocalization analysis, overlap was determined by drawing small circles (610 nm) around NPY-EGFP granules in the green image and transferring the circles to the red image. Colocalization was scored positive when a red dot was found within the circle. The percent colocalization between NPY-EGFP and FM4-64 was determined in single cells, and these values were then averaged.

To locate exocytic events, movies of the entire cell were scanned by eye for brightening events. The time and location of each fusion event in a cell were cataloged, and small regions (3.11 × 3.11 μm) containing each granule were excised as a ministack. As described (7), onset of exocytosis was defined as the first frame showing a visible increase in EGFP fluorescence over background. Regions of interest were centered on the brightest pixel of the granule during the first frame of exocytosis. In two-color experiments, regions located in the green image were transferred to the corresponding coordinates in the red image, and the red-channel ministacks were excised for analysis.

Two methods were used to measure granule fluorescence. In the first, fluorescence from EGFP or mRFP was measured in a 610-nm-diameter circle centered on the granule, and the fluorescence in a concentric annulus (1.2-μm outer diameter) was subtracted as local background. FM4-64 fluorescence was determined similarly except that background was measured in the entire surrounding area (3.11 × 3.11 μm square) to average out disturbances from abundant non-granule organelles. The second method was used to determine EGFP-phogrin fluorescence in granules where NH_4Cl application caused large fluorescence changes in neighboring granules, some located in the 1.2-μm diameter annulus. To isolate better the fluorescence of a granule from that of its neighbors, we used a program written in MATLAB and kindly provided by D. Perrais (University of Bordeaux 2, Bordeaux, France). The program fitted images in ministacks with the sum of an inclined plane, and two circularly symmetric Gaussian functions, one for the granule of interest and another for its nearest neighbor. The fit had nine free parameters, three each for the inclined plane (the fluorescence in the central pixel and the slopes in the x and y directions) and the two Gaussians (the amplitudes, widths, and center positions). The procedure isolated the granule of interest from the nearest surrounding granule. As the granule of interest moved within the region, its position was updated because it was a free parameter. The fluorescence of a granule was taken to be the amplitude of the Gaussian function fitted to that granule.

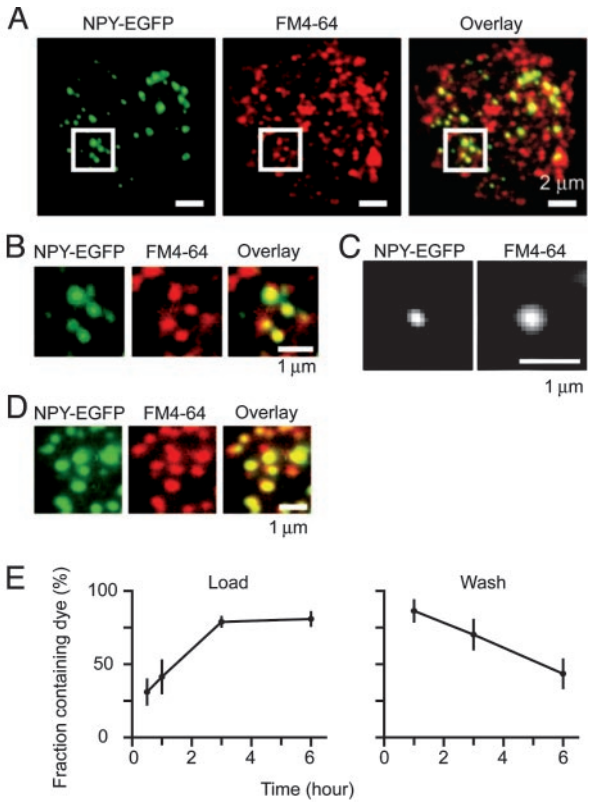

Fig. 1. Secretory granules accumulate the styryl dye FM4-64. (*A*) Evanescent field images of a PC12 cell transfected with NPY-EGFP (*Left*) and loaded with FM4-64 (*Center*); a merged image appears on the *Right*. (*B*) Magnified images of the regions marked with white boxes in *A*. (*C Left*) Square regions (1.5 × 1.5 μm) centered on single NPY-EGFP-containing granules were excised from green images and averaged (30 granules, three cells). (*Right*) As on the left for the same regions in the red channel. (*D*) NPY-EGFP-expressing cells were loaded with FM4-64 as in *A–C* but then ruptured with a jet of buffer solution. Patches of membrane remained, and a small region of one such patch is shown. (*E Left*) Uptake of FM4-64 by intact cells. Cells exposed to FM4-64 for various times were washed and then imaged. The fraction of granules containing FM4-64 is plotted against time in the presence of FM4-64 (*Left*). (*Right*) Loss of dye from intact cells. Cells were loaded with a 12-hr exposure to FM4-64, then washed, incubated for various times in dye-free solution, and finally imaged. Each point is the mean from at least 20 granules each in at least five cells.

Results

Secretory Granules Accumulate the Styryl Dye FM4-64. PC12 cells expressing the green fluorescent granule marker NPY-EGFP (7, 29) were cultured overnight in media containing the red lipidic styryl dye FM4-64 and then washed. They were then imaged with evanescent field fluorescence microscopy (27, 30), a technique that selectively images the plasma membrane and adjacent cytoplasm in the "footprint" where a cell adheres closely to the coverslip. The images in Fig. 1*A* show numerous green dots, each a secretory granule, as well as red dots representing organelles containing FM4-64. There were more red dots than green dots (shown in the merged image), indicating that FM4-64 does not label granules specifically. Nonetheless, some FM4-64-labeled structures clearly contained also NPY-EGFP, suggesting that the dye also enters granules. This result is seen better at higher magnification (1*B*).

Because of the high density of FM4-64-labeled structures, we tested whether the colocalization of NPY-EGFP and FM4-64

was due to random overlap. Images of 30 NPY-EGFP granules were excised and added together, and the same was done with the corresponding region from the red channel (Fig. 1*C*). Both panels show a dot in the center, demonstrating that FM4-64 was strongly enriched at granule sites and that colocalization was not an artifact of probe density. The higher background in the FM4-64 image arises from the staining of other organelles.

To test whether FM4-64 stained the outer or inner leaflet of the granule membrane, cells were ruptured with a strong jet of buffer from a perfusion pipette. Plasma membrane patches that remained stuck to the coverslip contained green granules (31), and, even minutes after cell rupture, most or all of the granules still contained FM4-64 (1D). Because styryl dyes desorb from membranes into a surrounding solution within seconds (32), FM4-64 must have been trapped within the lumen of the granules.

To determine the rate of FM uptake by granules, we incubated NPY-EGFP-transfected cells with FM4-64 and then counted the number of green granules containing FM4-64 over a period of hours. FM4-64 labeled 80% of the green granules within 3 hr (Fig. 1*E Left*). FM4-64 was subsequently lost from most granules after a 6-hr wash in dye-free medium (Fig. 1*E Right*). Evidently, FM4-64 enters granules reversibly.

Granules Lose FM4-64 During Exocytosis. To test whether FM4-64 escapes from granules during exocytosis, we imaged individual granules labeled with NPY-EGFP and FM4-64. Fig. 2*A* shows video stills of a single granule containing both NPY-EGFP and FM4-64 (Movie 1, which is published as supporting information on the PNAS web site). As before (7), exocytosis caused NPY-EGFP first to brighten and then to dim. The granule brightened as it connected with the external space and its internal pH rose, and as NPY-EGFP was secreted against the coverslip. Granules then dimmed in small fractions of a second as some or all of their NPY-EGFP diffused away. FM4-64 fluorescence dimmed just as rapidly, indicating rapid loss of the dye from the granule. The experiment is analyzed in Fig. 2 *B* and *C* where the fluorescence from both fluorophores is plotted against time, with average results shown in Fig. 2 *D* and *E*. As soon as NPY-EGFP brightened, FM4-64 fluorescence declined. Thus, on the time scale of our measurements (30 ms per frame), FM4-64 started to leave as soon as the lumen of the granule established continuity with the extracellular space. As a control, neighboring granules that did not show a change in NPY-EGFP fluorescence and did not undergo exocytosis did not exhibit a change in the FM4-64 signal (Fig. 2*E*).

FM4-64 Spreads into the Plasma Membrane. In hippocampal synaptic terminals, FM1-43, a yellow homologue of FM4-64, was found to leave synaptic vesicles by desorption from the vesicle membrane and loss into the external fluid, a process that takes of the order of a second (13, 17). In retinal bipolar neurons, by contrast, dye leaves synaptic vesicles in <10 ms by lateral diffusion into the plasma membrane (23). In terms of speed, the escape of FM4-64 from granules is more reminiscent of bipolar than of hippocampal neurons because it is complete in <100 ms (Fig. 2*E*). When an exponential function was fitted to the drop in fluorescence seen in Fig. 2*E*, the time constant was 45 ms. For two reasons, even this small value is substantially overestimated. First, Fig. 2*E* is an average obtained from sequences temporally aligned to the moment of fusion, and such alignment is accurate only to within the exposure time for a single image. Second, the moment of exocytosis is expected to occur randomly at any time during the 30-ms acquisition time of a single image. Even if alignment were perfect and FM4-64 left instantly, the resulting change in fluorescence would seem to take two frames, not much less than observed in Fig. 2*E*. Most probably, the discharge of FM4-64 was complete within 30 ms, the exposure time of a single image.

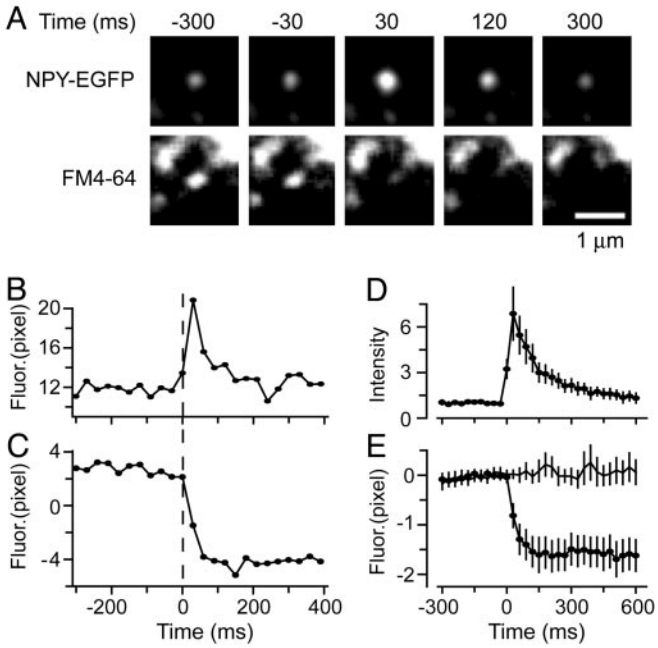

Fig. 2. Granules lose FM4-64 during exocytosis. (*A*) Images taken from a video clip of a granule containing NPY-EGFP (*Upper*) and FM4-64 (*Lower*) during exocytosis. The first frame wherein NPY-EGFP brightened measurably was taken to mark the start of exocytosis and the time origin. Granules usually continued to brighten, reaching maximal brightness 30 ms later. For clarity, each pixel value was multiplied by 10 and the resulting images were low-pass filtered (3 pixels), but all analysis was done before multiplication and filtering. (*B*) Plot of the NPY-EGFP fluorescence of the granule in *A*, measured in a 610-nm-diameter circle. Fluorescence in a concentric annulus was subtracted as background. Fusion is taken to have occurred at the first sign of the granule getting brighter, thus defining the time origin. (*C*) FM4-64 fluorescence at the same site, corrected for background using a square area (see *Methods*). (*D*) NPY-EGFP fluorescence traces as in *B* were divided by their average value over the last 150 ms before fusion and then averaged (25 granules, four cells). (*E*) FM4-64 fluorescence of the granules analyzed in *D*. Traces as in *C* had their average value during the last 150 ms before exocytosis subtracted. The results were then averaged and are shown by the line with filled circles. Line without symbols is fluorescence at sites of neighboring granules that did not undergo exocytosis (25 granules, four cells).

We wondered whether the dimming of FM4-64 in exocytic granules occurred by loss of the dye into the imaging buffer, or by spread into the plasma membrane. This point was tested by measuring the fluorescence of a large region centered on a granule (Fig. 3*A*). The larger region did in fact dim over the course of the recording, but this result was likely due to photobleaching because it occurred continuously and was temporally uncorrelated with exocytosis. At the moment of exocytosis, there was instead an increase in fluorescence (open circles in Fig. 3*A*). The increase was small when our laser beam was s-polarized (33) and generated an evanescent field oscillating in parallel to the plasma membrane. It was much larger with a p-polarized beam (filled circles) generating an evanescent field with a component oscillating in a direction perpendicular to the plasma membrane. This direction is especially favorable for exciting styryl dyes in the plasma membrane (23). Fig. 3*A* indicates that exocytosis causes styryl dye to spread into the plasma membrane rather than being lost. First, the total amount of fluorescence increased. Second, the increase required p-polarized light, which excites FM1-43 more effectively when the dye is located in the planar plasma membrane than in a spherical secretory vesicles (23). Spread into the plasma membrane could be observed directly when multiple exocytic events are averaged

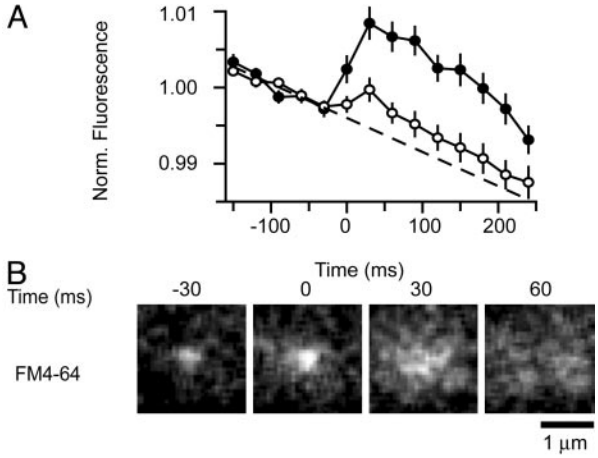

Fig. 3. Effect of polarization. (*A*) FM4-64 fluorescence in larger regions (3.11 × 3.11 μm square) centered over granules undergoing exocytosis. Illumination with either s-polarized (open circles, 25 granules, four cells) or p-polarized light (filled circles, 20 granules, five cells). Individual fluorescence traces were aligned to the moment of exocytosis as determined from the NPY-EGFP signal (see Fig. 2) and divided by their mean value during the last 150 ms before fusion. The results were then averaged. The dashed line was fitted to the traces 150 ms before exocytosis, and its slope is attributed to photobleaching. No background subtraction was applied to the images other than removing the electronic offset of the camera in total darkness. (*B*) Image sequences were acquired as in Fig. 2*A* but with p-polarized light to highlight dye located in the plasma membrane. To cancel out the fluorescence from neighboring structures not undergoing exocytosis, five sequential frames beginning 300 ms after exocytosis were averaged together, and the result was subtracted from each sequence. The sequences thus treated were added together (20 granules, five cells) and subjected to 3-pixel low-pass filtering.

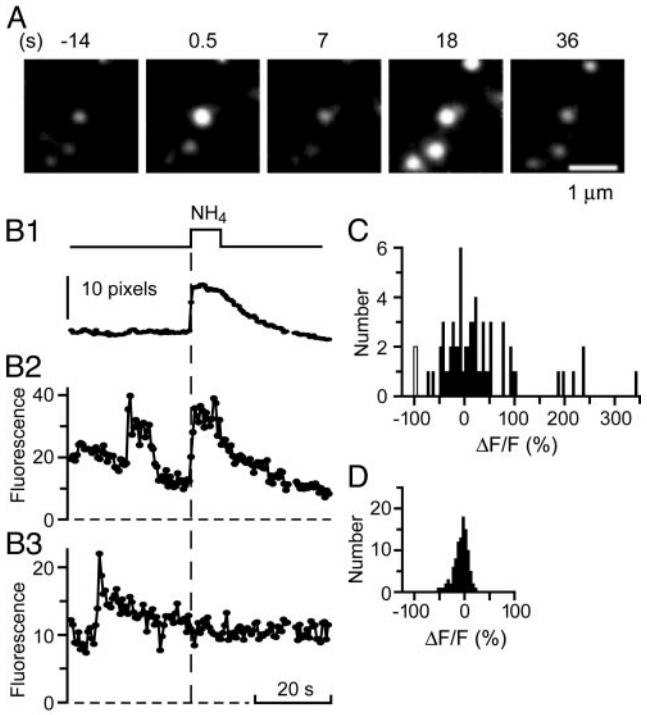

Fig. 4. Some granules reacidify after exocytosis. (*A*) EGFP-phogrin-labeled granule brightens during exocytosis, dims, and then rebrightens during superfusion with 50 mM NH_4Cl. Images processed as in Fig. 2*A* for visual clarity. (*B1*) Fluorescence from granules that failed to undergo exocytosis in that cell. Background subtraction is as in Fig. 2*B*; the results represent the average of six granules. (*B2*) Fluorescence of the granule in the center of the images in *A*, calculated by fitting Gaussian functions (see *Methods*). (*B3*) As in *B2*, but in a granule that underwent exocytosis but did not brighten when NH_4Cl was added. (*C*) NH_4Cl-induced fluorescence changes were determined as in *B2* and *B3*. Gaussians were fitted to two images of each granule, one an average over the last 2.5 s before superfusion, the other over a 2.5-s interval starting 1–2 s after NH_4Cl was applied. Each value in *C* is the difference, ΔF, between the amplitudes of the two Gaussians, given as a percentage of the amplitude (F) before NH_4Cl was applied. NH_4Cl was applied 5 to 47 s after exocytosis (64 granules in 19 cells). The two events with $\Delta F/F = -100\%$ refer to granules where the fitting routine failed for the images taken during the NH_4Cl application. (*D*) As in *C* except that cells were not stimulated, and the buffer used for superfusion lacked NH_4Cl.

(Fig. 3*B* and Movie 2, which is published as supporting information on the PNAS web site).

Recapture of Granules After Exocytosis. To test whether granules resealed, we used the granule membrane protein phogrin with EGFP attached on its luminal domain. EGFP-phogrin serves as a probe of the intragranular pH (34). Like NPY-EGFP, EGFP-phogrin brightened on exocytosis as granules lost acid and then dimmed again, as in the first three panels of Fig. 4*A*. Dimming may indicate reacidification of the granule lumen. This possibility was tested by superfusing the cell with imaging buffer containing NH_4Cl. NH_4Cl collapses proton gradients across internal membranes (34), and will cause all EGFP-phogrin in acidic compartments to brighten (34). Four granules lit up. Three were virgin granules, and the fourth was the one that had undergone exocytosis (Fig. 4*A* and Movie 3, which is published as supporting information on the PNAS web site). Evidently that granule had resealed, and most or all its postexocytic dimming was due to reacidification. The experiment is analyzed in Fig. 4*B*. Fig. 4*B1* plots the fluorescence of virgin granules as NH_4Cl was applied and withdrawn and marks the time course of NH_4Cl action. Fig. 4*B2* plots the fluorescence of the granule that underwent exocytosis and then resealed, and Fig. 4*B3* that of another granule that remained open. In similar experiments, 32 of 78 granules brightened visibly when NH_4Cl was applied whereas 32 others failed to do so. No verdict could be reached on the remaining 14 granules. All but one became invisible before application of NH_4Cl. These granules either lost their phogrin before NH_4Cl was applied or had resealed and retracted into the cytosol. In one case, the granule's image merged with that of another. The median time between fusion and NH_4Cl application was 17 s (5–47 s for granules that resealed and 6–43 s for granules that did not).

We wished to quantify the effect of NH_4Cl on the fluorescence of postexocytic granules. The main difficulty was that postexocytic granules were often close to virgin granules that had not undergone exocytosis but also brightened strongly. To minimize the disturbance from virgin granules, we fitted Gaussian functions both to the postexocytic granule and to its nearest virgin neighbor (see *Methods*). The amplitude of the Gaussian fitted to the postexocytic granule was taken to represent that granule's fluorescence. Measurements were made just before the application of NH_4Cl and again while NH_4Cl was present. The difference between the two values was expressed as the fractional fluorescence change ($\Delta F/F$) and varied strongly among postexocytic granules (Fig. 4*C*). Many such granules brightened, presumably because they had restored their pH gradient after they had resealed. Others did not strongly change their fluorescence, and still others apparently dimmed further.

As a control, the analysis was carried out also on granules that had undergone no exocytosis and were mock-perfused with imaging buffer that lacked NH_4Cl. The $\Delta F/F$ varied much less (Fig. 4*D*). Most such granules dimmed, presumably because of photobleaching or because they moved some distance into the cytosol. $\Delta F/F$ was usually negative (median -5%). In none of

100 granules was $\Delta F/F > 22\%$. We next tested how the brightening of virgin neighbors influenced our analysis. We added to the images of the cells analyzed in Fig. 4*D* the image of an artificial granule, represented by a Gaussian profile of constant position. Its amplitude (13 pixel units) was similar to the mean amplitude measured for postexocytic granules before NH_4Cl was applied. When $\Delta F/F$ was determined for the artificial granule, the median value was $\Delta F/F = -7\%$ (mean $-$ 8%, $n =$ 100). Evidently, our fitting procedure underestimated the NH_4Cl-induced brightening of postexocytic granules. The error was larger when the artificial granule was dimmer. When its amplitude was similar to that of the dimmest postexocytic granules (6 pixel units), the median value of $\Delta F/F$ was -25%, with 2 of 9 values less than -50%. Evidently, our analysis becomes unreliable when postexocytic granules are dim and close neighbors brighten strongly. This fact contributes to the apparent strong dimming of some postexocytic granules in Fig. 4*C*.

To summarize, virgin granules never brightened by >22% when no NH_4Cl was applied. When NH_4Cl was applied, virgin granules brightened and caused errors, but these tended to make $\Delta F/F$ too negative and hence to mask rather than accentuate the brightening of postexocytic granules. Thus, we consider that any postexocytic granule brightening by >25% did so because NH_4Cl collapsed its proton gradient. Indeed, in all of 23 such granules, the brightening was also visually apparent. We consider that, at least in this subset, all granules resealed. In 26 other postexocytic granules, $\Delta F/F < -5\%$ in Fig. 4*D*. We consider that these granules remained open.

Loss of FM4-64 Is Independent of Recapture. When synaptic vesicles are found to undergo kiss-and-run exocytosis, the fusion pore is a barrier to the exchange of styryl dyes (17). To test whether the same applies also to resealing granules, EGFP-phogrin-expressing cells were loaded with FM4-64 and imaged in two colors simultaneously. Granules were divided into two groups based on their response to NH_4Cl, containing the granules that resealed (filled circles) and those that remained open (open circles in Fig. 5 *A* and *B*). Both groups showed a similar loss of EGFP-phogrin fluorescence, indicating that resealing granules dim by acidification about as fast as open granules lose EGFP-phogrin. More importantly, resealing granules lost as much FM4-64 as open granules. Evidently, granules in PC12 cells lose FM4-64 before they reseal.

Granules Retain More Phogrin When They Reseal than When They Stay Open. In hippocampal neurons, it was found that the membrane protein synaptobrevin remained in synaptic vesicles that resealed after exocytosis (18). To test how much phogrin remains in granules after exocytosis (7, 24, 25), phogrin was labeled with mRFP (26) at its cytosolic end, yielding phogrin-mRFP. Insensitive to the intragranular pH, the mRFP in this construct is expected to report the amount of phogrin remaining in the granule. Along with phogrin-mRFP, cells expressed NPY-EGFP to mark the moment of exocytosis. Granules lost phogrin-mRFP fluorescence to variable extents. Fig. 5 *C1* and *C2* shows two extreme cases. One granule lost essentially none (Fig. 5*C1*) and another essentially all (Fig. 5*C2*). On average, granules retained about half their phogrin-mRFP during the first 20 s after exocytosis (Fig. 5*D*). This amount is less than in earlier work (7) that used phogrin labeled with DsRed, a protein known to form tetramers (35).

Do granules retain more phogrin when they reseal? This point was tested in EGFP-phogrin-expressing granules analyzed as in Fig. 4. We divided the fluorescence of each granule in the presence of NH_4Cl by that measured just after exocytosis. The resulting ratio is expected to be proportional to the fraction remaining in the granule. It was significantly less ($P < 0.0001$) in granules that remained open (Fig. 5*D*, open bar) than in those that resealed (Fig. 5*D*, filled bar). Hence the loss of phogrin-mRFP in Fig. 5*D* is mostly due to granules that remained open. This finding suggests that resealing granules lose little or no phogrin, in some ways similar to synaptic vesicles that retain synaptobrevin when they undergo kiss-and-run (18).

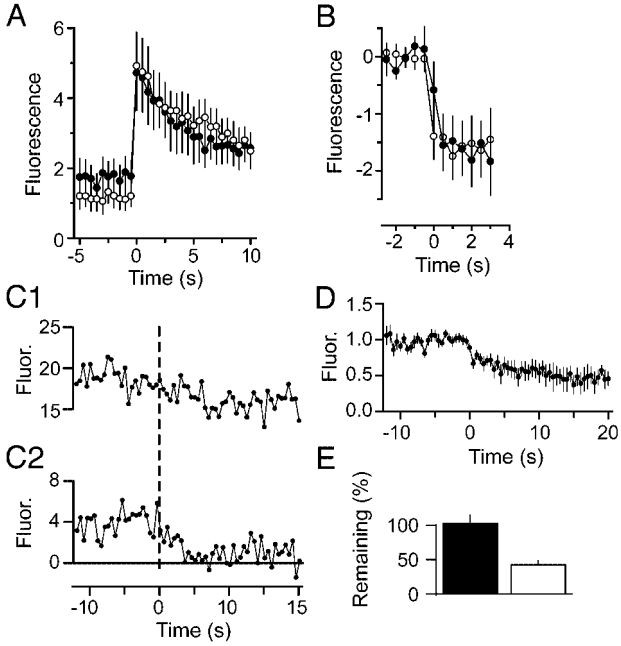

Fig. 5. Resealed granules lose FM4-64 but retain phogrin. (*A* and *B*) Fluorescence of EGFP-phogrin and of FM4-64 in granules that were grouped according to their response to NH_4Cl. Open granules had $\Delta F/F < -5\%$, the median in Fig. 4*D* (open circles, 12 granules in six cells). Resealed granules passed two tests. They brightened visibly in response to NH_4Cl, and had $\Delta F/F$ >25%, a value larger than any granule in Fig. 4*D* (filled circles, 13 granules in seven cells). In *A*, fluorescence traces were analyzed as in Fig. 2*B* except that EGFP-phogrin rather than NPY-EGFP was used to mark the moment of exocytosis. The resulting traces were then averaged. In B, FM4-64 fluorescence traces were analyzed as in Fig. 2 *C* and *E*. (*C1* and *C2*) Fluorescence of two granules containing mRFP, analyzed as in Fig. 2*B* in cells also expressing NPY-EGFP. Time origin is the moment of fusion as reported by NPY-EGFP. (*D*) Traces as in *C1* and *C2* were divided by their average value over the last 2.5 s before fusion, and the results were averaged (10 granules in eight cells). (*E*) Analysis of a subset of the data shown in Fig. 4C. The granule fluorescence during NH_4Cl perfusion was divided by that measured similarly but from images averaged over the first 1.5 s after exocytosis. Resealing (filled bar, $n =$ 17) or lack thereof (open bar, $n = 15$) was judged by the criteria used in (*A* and *B*). The dataset includes granules not stained with FM4-64 but excludes those exposed to NH_4Cl >20 s after exocytosis. Values are different with $P < 0.0001$ by ANOVA.

Discussion

Here, we used a lipid probe to test whether the bilayers of individual granules in PC12 cells merge with the plasma membrane. We found that styryl dye escaped from single granules after exocytosis, with dye loss largely being completed within the first 30 ms after fusion. As in synaptic vesicles of retinal bipolar cells (23), dye escaped by lateral diffusion into the plasma membrane. This finding provides evidence that the lipid bilayers of the granule and the plasma membrane become continuous within <30 ms after exocytosis. We further used the granule membrane marker EGFP-phogrin to test whether individual granules reseal after exocytosis (7). By this method, nearly half of all granules were found to do so. When EGFP-phogrin and FM4-64 were imaged simultaneously, FM4-64 was seen to escape as readily from granules that resealed as it did from those that

did not. Apparently, granules merge their bilayers with the plasma membrane, but this fact does not prevent half of them from resealing later. As soon as the bilayers connect, the soluble SNARE molecules that have mediated fusion find themselves in the same membrane, and are free to form cis-complexes. These cis-complexes are so stable that their formation is essentially irreversible (36). As a consequence, the mechanism that reseals granules is unlikely to be the molecular reverse of fusion. Instead, resealing probably requires the recruitment of fission-mediating molecules, such as dynamin (6, 37, 38).

It has been proposed that synaptic vesicles also can reseal after they release transmitter (20, 39). In this model of exocytosis, the vesicle does not exchange membrane components with the plasma membrane (21). This idea has recently gained considerable attention under the name kiss-and-run exocytosis (40–42). Some of the strongest evidence supporting kiss-and-run has been obtained by measuring the loss of membrane dyes such as FM1-43 from synaptic vesicles. Specifically, hippocampal synaptic terminals and the neuromuscular junction of flies have been found to release styryl dyes from vesicles slowly and incompletely during exocytosis (13, 14, 16, 17). In addition, the rate and proportion of release were dependent on the desorption rate of the dye, suggesting that dye could not leave by lateral diffusion and instead must first unbind from the vesicle lumen and escape by the same route as neurotransmitter (13, 17, 43). These studies imply that the bilayers of the vesicles and plasma membrane do not merge and suggest that fusion during kiss-and-run is incomplete. If so, the rapid resealing of synaptic vesicles may simply be the molecular reversal of exocytosis (14).

It might be useful to distinguish two phenotypes of vesicle recapture. In the kiss-and-run model, vesicles do not exchange membrane components with the plasma membrane. In contrast, granules in PC12 cells participate in a more complete form of fusion, allowing at least the lipid bilayer of granules to mix with the plasma membrane before they reseal. In other cells, even membrane proteins may escape into the plasma membrane until only the cavity of the granule remains. We propose to call this type of resealing "cavicapture," to distinguish it from kiss-and-run, with its emphasis on complete retention of membrane components (21).

We thank L. Kwan for technical assistance and Dr. S. Arch for helpful comments on the manuscript. This work was supported by National Institutes of Health Grants DK44239 and MH60600.

1. Fernandez, J. M., Neher, E. & Gomperts, B. D. (1984) *Nature* **312,** 453–455.
2. Spruce, A. E., Breckenridge, L. J., Lee, A. K. & Almers, W. (1990) *Neuron* **4,** 643–654.
3. Albillos, A., Dernick, G., Horstmann, H., Almers, W., Alvarez de Toledo, G. & Lindau, M. (1997) *Nature* **389,** 509–512.
4. Ales, E., Tabares, L., Poyato, J. M., Valero, V., Lindau, M. & Alvarez de Toledo, G. (1999) *Nat. Cell Biol.* **1,** 40–44.
5. Angleson, J. K., Cochilla, A. J., Kilic, G., Nussinovitch, I. & Betz, W. J. (1999) *Nat. Neurosci.* **2,** 440–446.
6. Holroyd, P., Lang, T., Wenzel, D., De Camilli, P. & Jahn, R. (2002) *Proc. Natl. Acad. Sci. USA* **99,** 16806–16811.
7. Taraska, J. W., Perrais, D., Ohara-Imaizumi, M., Nagamatsu, S. & Almers, W. (2003) *Proc. Natl. Acad. Sci. USA* **100,** 2070–2075.
8. Henkel, A. W. & Almers, W. (1996) *Curr. Opin. Neurobiol.* **6,** 350–357.
9. Klyachko, V. A. & Jackson, M. B. (2002) *Nature* **418,** 89–92.
10. Tse, A., Tse, F. W., Almers, W. & Hille, B. (1993) *Science* **260,** 82–84.
11. Zimmerberg, J., Blumenthal, R., Sarkar, D. P., Curran, M. & Morris, S. J. (1994) *J. Cell Biol.* **127,** 1885–1894.
12. Chernomordik, L. V., Frolov, V. A., Leikina, E., Bronk, P. & Zimmerberg, J. (1998) *J. Cell Biol.* **140,** 1369–1382.
13. Klingauf, J., Kavalali, E. T. & Tsien, R. W. (1998) *Nature* **394,** 581–585.
14. Stevens, C. F. & Williams, J. H. (2000) *Proc. Natl. Acad. Sci. USA* **97,** 12828–12833.
15. Pyle, J. L., Kavalali, E. T., Piedras-Renteria, E. S. & Tsien, R. W. (2000) *Neuron* **28,** 221–231.
16. Zakharenko, S. S., Zablow, L. & Siegelbaum, S. A. (2002) *Neuron* **35,** 1099–1110.
17. Aravanis, A. M., Pyle, J. L. & Tsien, R. W. (2003) *Nature* **423,** 643–647.
18. Gandhi, S. P. & Stevens, C. F. (2003) *Nature* **423,** 607–613.
19. Verstreken, P., Kjaerulff, O., Lloyd, T. E., Atkinson, R., Zhou, Y., Meinertzhagen, I. A. & Bellen, H. J. (2002) *Cell* **109,** 101–112.
20. Ceccarelli, B., Hurlbut, W. P. & Mauro, A. (1973) *J. Cell Biol.* **57,** 499–524.
21. Valtorta, F., Meldolesi, J. & Fesce, R. (2001) *Trends Cell Biol.* **11,** 324–328.
22. Sankaranarayanan, S. & Ryan, T. A. (2000) *Nat. Cell Biol.* **2,** 197–204.
23. Zenisek, D., Steyer, J. A., Feldman, M. E. & Almers, W. (2002) *Neuron* **35,** 1085–1097.
24. Ohara-Imaizumi, M., Nakamichi, Y., Tanaka, T., Katsuta, H., Ishida, H. & Nagamatsu, S. (2002) *Biochem. J.* **363,** 73–80.
25. Tsuboi, T., Zhao, C., Terakawa, S. & Rutter, G. A. (2000) *Curr. Biol.* **10,** 1307–1310.
26. Campbell, R. E., Tour, O., Palmer, A. E., Steinbach, P. A., Baird, G. S., Zacharias, D. A. & Tsien, R. Y. (2002) *Proc. Natl. Acad. Sci. USA* **99,** 7877–7882.
27. Steyer, J. A. & Almers, W. (2001) *Nat. Rev. Mol. Cell Biol.* **2,** 268–275.
28. Merrifield, C. J., Feldman, M. E., Wan, L. & Almers, W. (2002) *Nat. Cell Biol.* **4,** 691–698.
29. Lang, T., Wacker, I., Steyer, J., Kaether, C., Wunderlich, I., Soldati, T., Gerdes, H. H. & Almers, W. (1997) *Neuron* **18,** 857–863.
30. Axelrod, D. (2001) *J. Biomed. Opt.* **6,** 6–13.
31. Avery, J., Ellis, D. J., Lang, T., Holroyd, P., Riedel, D., Henderson, R. M., Edwardson, J. M. & Jahn, R. (2000) *J. Cell Biol.* **148,** 317–324.
32. Ryan, T. A., Smith, S. J. & Reuter, H. (1996) *Proc. Natl. Acad. Sci. USA* **93,** 5567–5571.
33. Sund, S. E., Swanson, J. A. & Axelrod, D. (1999) *Biophys. J.* **77,** 2266–2283.
34. Miesenbock, G., De Angelis, D. A. & Rothman, J. E. (1998) *Nature* **394,** 192–195.
35. Baird, G. S., Zacharias, D. A. & Tsien, R. Y. (2000) *Proc. Natl. Acad. Sci. USA* **97,** 11984–11989.
36. Hayashi, T., McMahon, H., Yamasaki, S., Binz, T., Hata, Y., Sudhof, T. C. & Niemann, H. (1994) *EMBO J.* **13,** 5051–5061.
37. Artalejo, C. R., Henley, J. R., McNiven, M. A. & Palfrey, H. C. (1995) *Proc. Natl. Acad. Sci. USA* **92,** 8328–8332.
38. Graham, M. E., O'Callaghan, D. W., McMahon, H. T. & Burgoyne, R. D. (2002) *Proc. Natl. Acad. Sci. USA* **99,** 7124–7129.
39. Torri-Tarelli, F., Grohovaz, F., Fesce, R. & Ceccarelli, B. (1985) *J. Cell Biol.* **101,** 1386–1399.
40. Fesce, R., Grohovaz, F., Valtorta, F. & Meldolesi, J. (1994) *Trends Cell Biol.* **4,** 1–4.
41. Jarousse, N. & Kelly, R. B. (2001) *Curr. Opin. Cell Biol.* **13,** 461–469.
42. Ryan, T. A. (2003) *Proc. Natl. Acad. Sci. USA* **100,** 2171–2173.
43. Ryan, T. A. (2001) *Curr. Opin. Neurobiol.* **11,** 544–549.